Journal of Alloys and Compounds 509 (2011) 10014–10019

Contents lists available at ScienceDirect

Journal of Alloys and Compounds

journal homepage: www.elsevier.com/locate/jallcom

Preparation and luminescence characterization of new carbonate ($Y_2(CO_3)_3{\cdot}nH_2O{:}Eu^{3+}$) phosphors via the hydrothermal route

Hau-Yun Chang, Fu-Shan Chen, Chung-Hsin Lu*

Department of Chemical Engineering, National Taiwan University, Taipei, Taiwan, ROC

ARTICLE INFO

Article history:
Received 21 January 2011
Received in revised form 29 July 2011
Accepted 1 August 2011
Available online 10 August 2011

Keywords:
Phosphor
Luminescence
Hydrothermal

ABSTRACT

A new Eu^{3+}-activated $Y_2(CO_3)_3{\cdot}nH_2O$ phosphor was successfully prepared via the hydrothermal process using urea as a reaction agent. $Y_2(CO_3)_3{\cdot}nH_2O{:}Eu^{3+}$ phosphors displayed an intense red emission at 615 nm due to the $^5D_0 \rightarrow {}^7F_2$ transition of Eu^{3+} ions under 254 nm excitation. The intensity of this emission was significantly increased with a rise in the hydrothermal temperatures. The study of photoluminescence properties demonstrated that Y^{3+} ions were replaced by Eu^{3+} ions in the host lattice at the 9-coordination sites. With an increase in heating temperatures, the morphology of $Y_2(CO_3)_3{\cdot}nH_2O{:}Eu^{3+}$ powders changed from a spherical to a rod-like shape. Calcination at elevated temperatures resulted in thermal decomposition of $Y_2(CO_3)_3{\cdot}nH_2O{:}Eu^{3+}$ to form $Y_2O_3{:}Eu^{3+}$. The formed $Y_2O_3{:}Eu^{3+}$ powder exhibited a rod-like morphology with an intense red emission.

1. Introduction

Inorganic phosphors have been extensively investigated recently because of their wide application to light emitting diodes (LEDs), plasma display panels (PDPs), and filed emission displays (FEDs) devices [1–3]. Rare-earth activated phosphors have attracted much attention due to their low toxicity, high chemical stability, high efficiency and strong VUV absorption. Hence, rare earth ions incorporated with aluminates [4], borates [5], and silicates [6] have been widely used as phosphors. Besides above materials, carbonate is another interesting host because of its thermal luminescence properties [7]. However, the luminescence properties of the carbonate-based phosphors are not investigated in details.

In this study, $Y_2(CO_3)_3{\cdot}nH_2O$ ($n = 2$–3) was utilized as a new host material to prepare a carbonate-based phosphor. The crystal structure of $Y_2(CO_3)_3{\cdot}nH_2O$ was first reported by Svanberg and Tenger. This material was redefined as a tengerite-(Y) structure by Nagoya, Kita and Ibaraki [8]. $Y_2(CO_3)_3{\cdot}nH_2O$ is an orthorhombic structure with space group $Bb2_1m$. Its lattice parameters are $a = 6.078$ Å, $b = 9.157$ Å, and $c = 15.114$ Å. The luminescence properties related to $Y_2(CO_3)_3{\cdot}nH_2O$ have not been reported in the literature.

Various techniques, such as the homogeneous precipitation method [9], the hydrothermal method [7], and the gel method [8], have been developed to prepare $Y_2(CO_3)_3{\cdot}nH_2O$. The reaction time of all above methods was needed at least for 2 days, and the crystallinity of obtained powders was insufficient. In order to overcome the drawbacks mentioned above, a new and fast synthesis route was developed in this study to prepare well-crystallized $Y_2(CO_3)_3{\cdot}nH_2O{:}Eu^{3+}$ in the hydrothermal system using urea as a precipitant. The hydrothermal process is an effective method to prepare crystallized ceramic powders. The hydrothermal process not only shortens the required reaction time, but also lowers the temperature for synthesizing ceramic powders [10–12]. Additionally, employing urea as a precipitant is reportedly crucial to synthesize carbonate-based powders with a uniform morphology [7].

In this study, $Y_2(CO_3)_3{\cdot}nH_2O{:}Eu^{3+}$ phosphor was prepared via the hydrothermal treatment. The luminescence properties of the prepared phosphors were investigated. The effects of hydrothermal temperatures on the luminescence properties and morphology of the obtained phosphors were discussed. Moreover, the thermal decomposition of $Y_2(CO_3)_3{\cdot}nH_2O{:}Eu^{3+}$ was also examined.

2. Experimental

2.1. Synthesis of $Y_2(CO_3)_3{\cdot}nH_2O{:}Eu^{3+}$ via the hydrothermal method

$Y_2(CO_3)_3{\cdot}nH_2O{:}Eu^{3+}$ phosphors were prepared via the hydrothermal reaction. Y_2O_3 (99.99%) and Eu_2O_3 (99.9%) were dissolved in concentrated nitric acid. The doping amount of Eu^{3+} ions was set to 5 mol% with respect to Y^{3+} ions. The total concentration of metal ions was adjusted to 0.05 M. The pH value of this solution was increased to be 7 via adding NH_4OH. A clear solution was obtained under heating and stirring at 80 °C for 2 h. Then a proper amount of urea was added into the solution with stirring for 2 h. The ratio of urea to metal ions (Y^{3+} and Eu^{3+}) was set to the value of 20:1. The resultant solution was transferred into a Teflon-bottled stainless steel autoclave. The volume of the autoclave was 30 ml. Besides, the liters of the solution charged into the autoclave were 24 ml. The autoclave was heated at temperatures

* Corresponding author. Tel.: +886 2 23651428; fax: +886 2 23623040.
E-mail address: chlu@ntu.edu.tw (C.-H. Lu).

0925-8388/$ – see front matter © 2011 Published by Elsevier B.V.
doi:10.1016/j.jallcom.2011.08.013

ranging from 90 °C to 210 °C for 12 h. $Y_2(CO_3)_3{\cdot}nH_2O{:}Eu^{3+}$ phosphors were obtained after the precipitates were washed with deionized water and dried in a vacuum oven.

2.2. Characterization

The X-ray diffraction patterns of the obtained powder were examined using a X-ray diffractometer (MAC Science M03XHF). The morphology and particle size of obtained powders were analyzed via a scanning electron microscope (SEM, Hitachi S-800). The photoluminescence spectra of the phosphors were obtained using a fluorescence spectrophotometer (Hitachi, F-4500) at room temperature. A 150 W xenon lamp was employed as the excitation light source. Thermal analysis of the prepared powders was performed with TG–DTA instruments (Rigaku TG8120). The samples were heated in air from room temperature to 800 °C at a heating rate of 10 °C min^{-1}.

3. Results and discussion

3.1. Effects of heating temperatures on the structure and morphology of $Y_2(CO_3)_3{\cdot}nH_2O{:}Eu^{3+}$ phosphors

$Y_2(CO_3)_3{\cdot}nH_2O{:}Eu^{3+}$ phosphors prepared at the different hydrothermal temperatures were characterized by XRD. The obtained results are presented in Fig. 1. After heating at 90 °C, a small amount of $Y_2(CO_3)_3{\cdot}nH_2O{:}Eu^{3+}$ was formed as seen in Fig. 1(a). After heating at 130 °C, the amount of crystallized $Y_2(CO_3)_3{\cdot}nH_2O{:}Eu^{3+}$ powders was increased (Fig. 1(b)). After heating at 170 and 210 °C (Fig. 1(c) and (d)), well-crystallized $Y_2(CO_3)_3{\cdot}nH_2O{:}Eu^{3+}$ powders with space group $Bb2_1m$ were obtained. All diffraction peaks were in agreement with that reported in ICDD No. 89-1462. The lattice parameters of $Y_2(CO_3)_3{\cdot}nH_2O{:}Eu^{3+}$ heated at 210 °C were calculated. The lattice parameters were $a = 6.056$ Å, $b = 9.132$ Å and $c = 15.016$ Å. In comparison to the homogeneous precipitation method, the requiring time for synthesizing $Y_2(CO_3)_3{\cdot}nH_2O{:}Eu^{3+}$ powders via this route was markedly shortened.

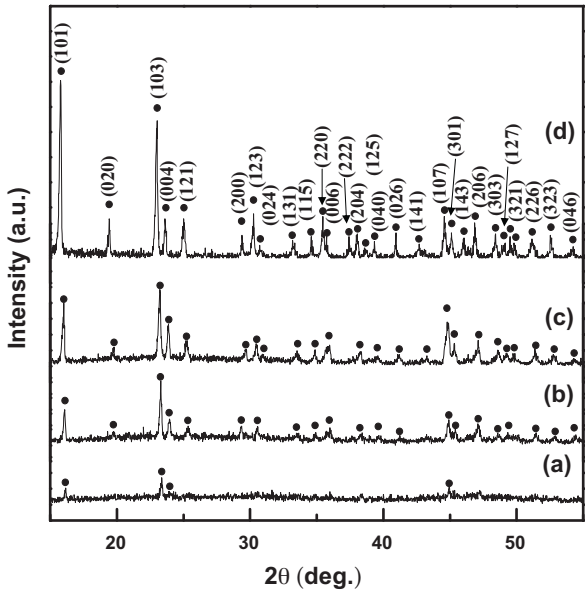

Fig. 1. X-ray diffraction patterns of $Y_2(CO_3)_3{\cdot}nH_2O{:}Eu^{3+}$ phosphors prepared via the hydrothermal process at (a) 90 °C, (b) 130 °C, (c) 170 °C and (d) 210 °C for 12 h.

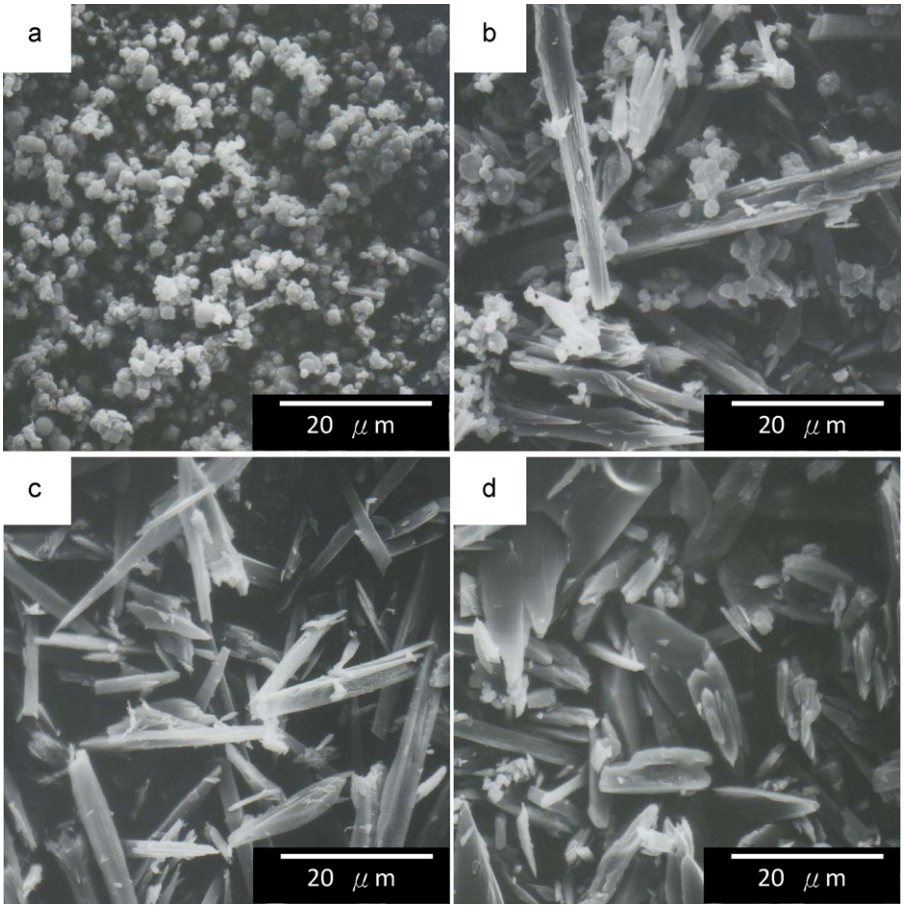

Fig. 2. Scanning electron microscope images of $Y_2(CO_3)_3{\cdot}nH_2O{:}Eu^{3+}$ phosphors prepared via the hydrothermal process at (a) 90 °C, (b) 130 °C, (c) 170 °C and (d) 210 °C for 12 h.

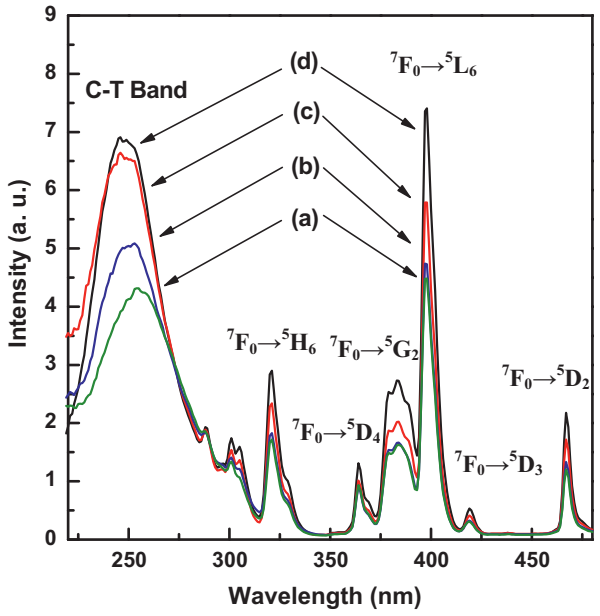

Fig. 3. Excitation spectra of $Y_2(CO_3)_3{\cdot}nH_2O{:}Eu^{3+}$ phosphors prepared via hydrothermal process at (a) 90 °C, (b) 130 °C, (c) 170 °C and (d) 210 °C.

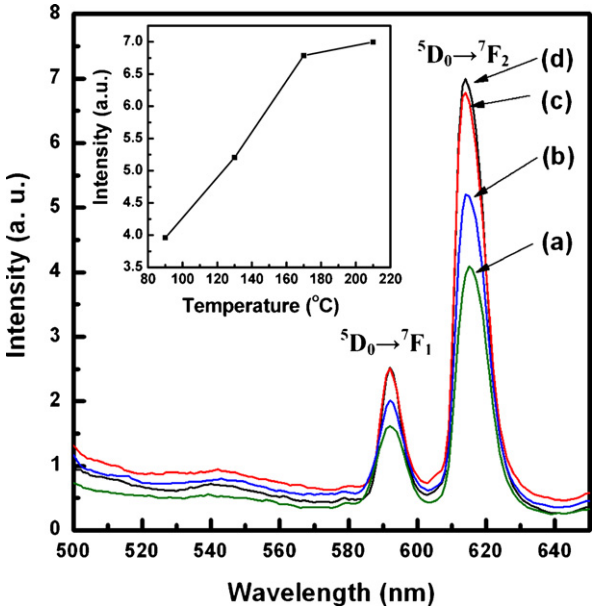

Fig. 4. Emission spectra of $Y_2(CO_3)_3{\cdot}nH_2O{:}Eu^{3+}$ phosphors prepared via hydrothermal process at (a) 90 °C, (b) 130 °C, (c) 170 °C and (d) 210 °C. Inset: dependence of emission intensity on heating temperatures.

In this study, the urea-based hydrothermal process was used for the formation of $Y_2(CO_3)_3{\cdot}nH_2O{:}Eu^{3+}$ phosphors. It is known that urea will be decomposed upon heating at higher than 70 °C to release ammonium and cyanate ions. In neutral or basic solutions, the cyanate ions will react with OH^- ions, and ammonia and carbonated ions are produced [13]. The hydrolysis reaction of urea can be expressed as below:

$$H_2N{-}CO{-}NH_2 \rightarrow NH_4^+ + OCN^- \quad (1)$$

$$OCN^- + OH^- + H_2O \rightarrow CO_3^{2-} + NH_3 \quad (2)$$

Hence, the yttrium carbonate phosphors were formed via reaction between Y^{3+} with CO_3^{2-} ions in the hydrothermal system. The overall chemical reactions can be described as below:

$$(2-x)Y^{3+} + xEu^{3+} + 3CO_3^{2-} + nH_2O \rightarrow Y_{2-x}Eu_x(CO_3)_3{\cdot}nH_2O \quad (3)$$

The SEM micrographs of $Y_2(CO_3)_3{\cdot}nH_2O{:}Eu^{3+}$ particles prepared via the hydrothermal route at different heating temperatures are shown in Fig. 2. The powder prepared at 90 °C exhibited a spherical shape, and the particle size was around 1–2 μm as seen in Fig. 2(a). When the temperature was increased to 130 °C, the shape of particles significantly changed. Some particles became to exhibit a rod-like shape. The diameter of the rod-like particles was in the range from 1 to 4 μm and the length was from 5 to 25 μm. Upon heating at 170 °C, all the particles exhibited a rod-like shape (Fig. 2(c)). The growth rate of an anisotropic material is tended to be promoted along a specific axis [14], thereby resulting in the formation of rod-like particles. When the temperature was increased to 210 °C, the size of rod-like particles further increased (Fig. 2(d)).

3.2. Photoluminescence properties of $Y_2(CO_3)_3{\cdot}nH_2O{:}Eu^{3+}$ phosphors

The excitation spectra (λ_{em} = 615 nm) of $Y_2(CO_3)_3{\cdot}nH_2O{:}Eu^{3+}$ phosphors prepared at 90, 130, 170, and 210 °C are illustrated in Fig. 3(a)–(d), respectively. $Y_2(CO_3)_3{\cdot}nH_2O{:}Eu^{3+}$ showed a broad excitation band in the 220–280 nm wavelength regions. This excitation band can be attributed to the $O^{2-} \rightarrow Eu^{3+}$ charge transfer transition. Several typical excitation peaks of Eu^{3+} ions were observed in the range of 300–500 nm. The intensities of the excitation peaks increased with increasing heating temperatures. These excitation peaks at 320, 364, 384, 396, 419, and 466 nm corresponded to the spectral transition of $^7F_0 \rightarrow {}^5H_6$, $^7F_0 \rightarrow {}^5D_4$, $^7F_0 \rightarrow {}^5G_2$, $^7F_0 \rightarrow {}^5L_6$, $^7F_0 \rightarrow {}^5D_3$, and $^7F_0 \rightarrow {}^5D_2$, respectively [15]. The dominant one was $^7F_0 \rightarrow {}^5L_6$ transition (396 nm).

Fig. 4 depicts the emission spectra of $Y_2(CO_3)_3{\cdot}nH_2O{:}Eu^{3+}$ phosphors prepared at different hydrothermal temperatures. The emission spectra were measured with an excitation wavelength of 254 nm. All obtained samples displayed $^5D_0 \rightarrow {}^7F_J$ (J = 1, 2) lines of Eu^{3+} ions [15]. The strongest emission was at 615 nm, corresponding to the $^5D_0 \rightarrow {}^7F_2$ transition. The inset in Fig. 4 indicates the emission intensities of $Y_2(CO_3)_3{\cdot}nH_2O{:}Eu^{3+}$ as a function of heating temperatures. The emission intensity of $Y_2(CO_3)_3{\cdot}nH_2O{:}Eu^{3+}$ was found to increase with an increase in heating temperatures because of the increased amount of $Y_2(CO_3)_3{\cdot}nH_2O$. The highest luminescence intensity was obtained when samples were heated at 210 °C under the hydrothermal treatment.

The emission peak at 615 nm was assigned to forced electric dipole transition of $^5D_0 \rightarrow {}^7F_2$ of Eu^{3+} ions. The $^5D_0 \rightarrow {}^7F_2$ transition is hypersensitive. The intensity of this transition strongly depends on the chemical environment. When emission peak of $^5D_0 \rightarrow {}^7F_2$ is dominant, indicateing Eu^{3+} ions occupy a site without inversion symmetry [16]. Hence, it clearly reveals that the structural symmetry of Y^{3+} was substituted by Eu^{3+} is low in the lattice. The position of emission wavelength was reported to vary slightly with Eu^{3+} coordination number [17]. Eu^{3+} located at 6-coordination, 9-coordination and 12-coordination sites will generate emission at 611, 615 and 625 nm, respectively. Hence, the main emission peak of $Y_2(CO_3)_3{\cdot}nH_2O{:}Eu^{3+}$ at 615 nm indicates the fact of the occupancy of Eu^{3+} ions at 9-coordination site. This behavior confirmed that Eu^{3+} ion replaced Y^{3+} ion in the host.

3.3. Differential thermal and thermogravimetric analyses of $Y_2(CO_3)_3{\cdot}nH_2O{:}Eu^{3+}$ phosphors

In order to understand the thermal stability of $Y_2(CO_3)_3{\cdot}nH_2O{:}Eu^{3+}$, the thermal analysis of obtained samples prepared at 170 °C under a hydrothermal treatment was preformed via TGA and DTA as shown in Fig. 5. The DTA curve

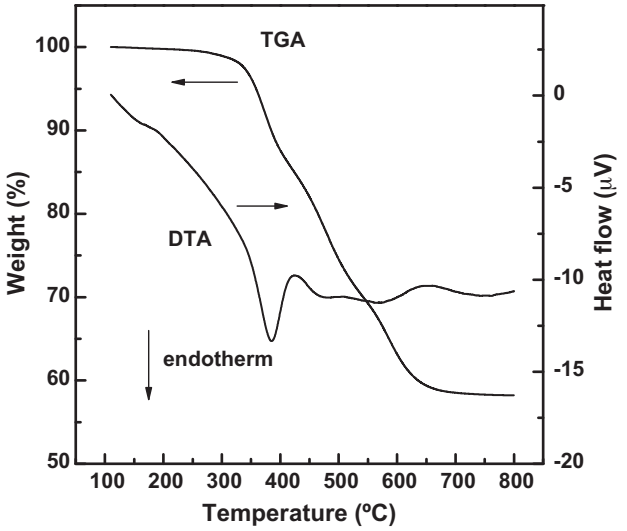

Fig. 5. TG/DTA curves of $Y_2(CO_3)_3{\cdot}nH_2O{:}Eu^{3+}$ phosphors. Heating rate: 10 °C min^{-1}.

revealed a strong endothermic peak at 385 °C, and a weak broad endothermic band ranging from 400 to 650 °C. The former reaction was considered to result from the dehydration and the decomposition of $Y_2(CO_3)_3{\cdot}2H_2O{:}Eu^{3+}$ structure [18], and the latter one is regarded as residual CO_2 released from the sample. In the TGA curve, the total weight lost after heat treatment up to 800 °C was around 41.8% of the initial weight. This loss percentage was close to the conversion loss of $Y_2(CO_3)_3{\cdot}nH_2O{:}Eu^{3+}$ to $Y_2O_3{:}Eu^{3+}$ when n was equal to 2. It was indicated that there were two molecules of water in this structure. This result was in agreement with the chemical formula of the tengerite-(Y) reported in the literature [19]. Additionally, there was no significant weight lost above 650 °C. This indicated that the reaction from $Y_2(CO_3)_3{\cdot}nH_2O{:}Eu^{3+}$ to oxide phase was complete after calcination at 650 °C.

3.4. Thermal decomposition of $Y_2(CO_3)_3{\cdot}nH_2O{:}Eu^{3+}$ phosphors

In order to understand the thermal decomposition process of $Y_2(CO_3)_3{\cdot}nH_2O{:}Eu^{3+}$ phosphors, the prepared samples prepared via the hydrothermal route at 170 °C were calcined at various temperatures for 2 h. Fig. 6 shows the X-ray diffraction patterns of the heated samples. Upon calcination at 400 °C, a weak peak belonging to Y_2O_3 phase was detected in the XRD patterns. It indicates that $Y_2(CO_3)_3{\cdot}nH_2O{:}Eu^{3+}$ phosphors were decomposed at this temperature, and $Y_2O_3{:}Eu^{3+}$ was formed. This result was agreement with the analysis of DTA curve. With a rise in the heating temperatures, the crystallinity of $Y_2O_3{:}Eu^{3+}$ became improved.

Fig. 7 presents the excitation spectra for $Y_2(CO_3)_3{\cdot}nH_2O{:}Eu^{3+}$ phosphors heated at 400, 500, 700, and 900 °C, respectively. The excitation spectra (λ_{em} = 611 nm) contained a large excitation band from 200 to 300 nm. This band had a maximum at 254 nm. It is assigned to the $O^{2-} \rightarrow Eu^{3+}$ charge-transfer (CT) band. The excitation spectra also contained several sharp lines in the region from 300 to 500 nm. These lines are attributed to the f–f transitions of Eu^{3+} ions [20].

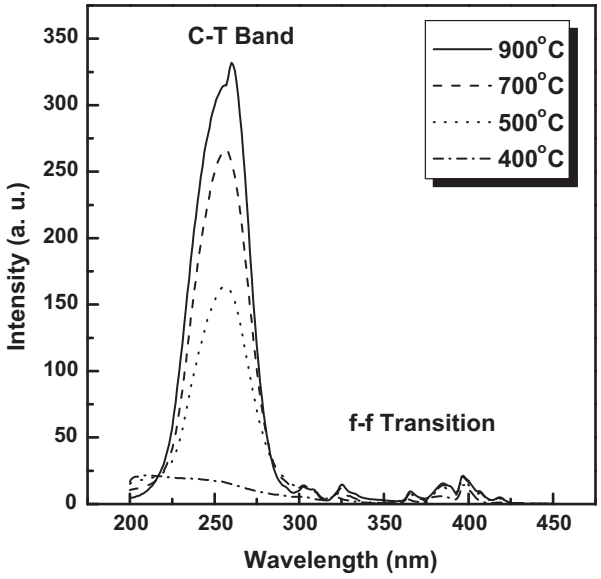

Fig. 7. Excitation spectra of $Y_2(CO_3)_3{\cdot}nH_2O{:}Eu^{3+}$ phosphors after calcination at 400, 500, 700, and 900 °C for 2 h.

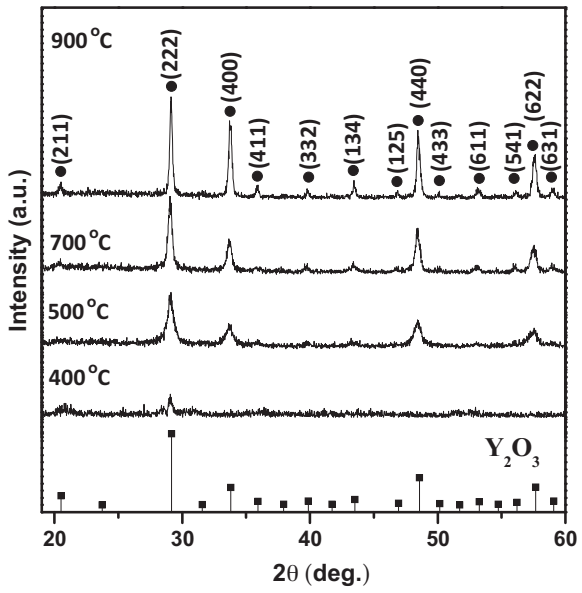

Fig. 6. X-ray diffraction patterns of $Y_2(CO_3)_3{\cdot}nH_2O{:}Eu^{3+}$ phosphors after calcination at the indicated temperatures for 2 h.

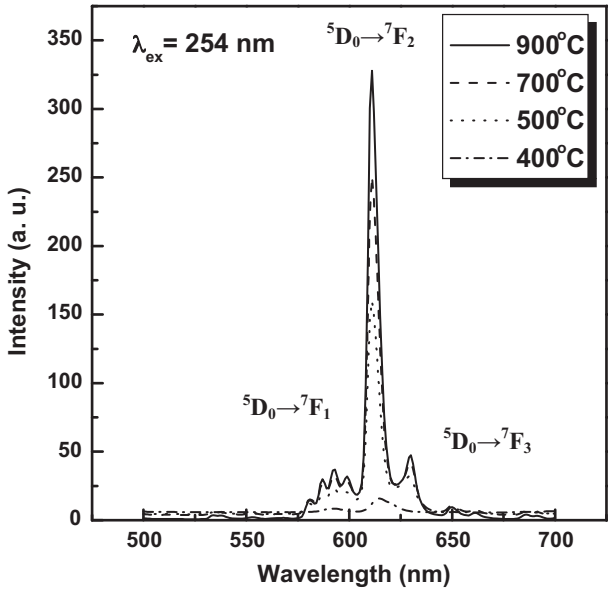

Fig. 8. Emission spectra of $Y_2(CO_3)_3{\cdot}nH_2O{:}Eu^{3+}$ phosphors after calcination at 400, 500, 700, and 900 °C for 2 h.

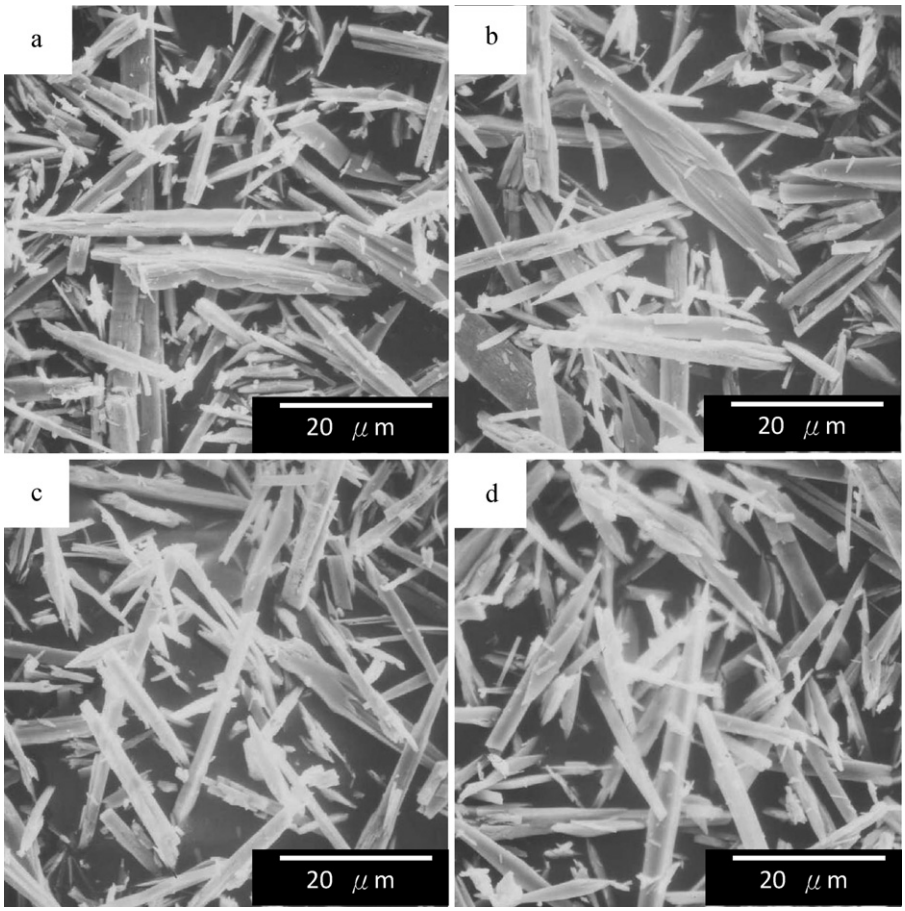

Fig. 9. Scanning electron microscope images of $Y_2(CO_3)_3{\cdot}nH_2O{:}Eu^{3+}$ phosphors after calcination at (a) 400, (b) 500, (c) 700, and (d) 900 °C for 2 h.

The emission spectra of $Y_2(CO_3)_3{\cdot}nH_2O{:}Eu^{3+}$ samples heated at elevated temperatures are presented in Fig. 8. Upon calcination at 400 °C, the obtained sample showed a weak emission peak in the spectrum. When the temperature was increased to 500 °C, the characteristic emission spectrum of $Y_2O_3{:}Eu^{3+}$ was displayed under 254 nm excitation. The main emission peak measured at 611 nm was due to the forbidden transition of $^5D_0 \rightarrow {}^7F_2$ of Eu^{3+} ions [21]. The emission intensity of the samples was increased monotonously with the increasing calcination temperatures. $Y_2O_3{:}Eu^{3+}$ phosphors displayed the highest emission intensity after calcination at 900 °C. The photoluminescence properties of $Y_2O_3{:}Eu^{3+}$ phosphors were found to be remarkably different from $Y_2(CO_3)_3{\cdot}nH_2O{:}Eu^{3+}$.

The SEM micrographs of $Y_2(CO_3)_3{\cdot}nH_2O{:}Eu^{3+}$ particles prepared at 170 °C under the hydrothermal reaction via heating at 400, 500, 700 and 900 °C are shown in Fig. 9(a)–(d), respectively. All heated powders had no significant change in morphology and exhibited a rod-like shape. The obtained results were similar to the powder as shown in Fig. 2(c). It is indicated the calcination had no influence on morphology of powders. On the other hand, it is worthwhile to note that the rod-like $Y_2O_3{:}Eu^{3+}$ phosphors can be easily obtained using $Y_2(CO_3)_3{\cdot}nH_2O{:}Eu^{3+}$ as a precursor. Base on the above results, it was confirmed that a new phosphor, $Y_2(CO_3)_3{\cdot}nH_2O{:}Eu^{3+}$, with an intense red emission was successfully obtained. The heating temperatures had significant effects on the morphology and the luminescence properties of $Y_2(CO_3)_3{\cdot}nH_2O{:}Eu^{3+}$ phosphors. Heating at elevated temperatures resulted in the thermal decomposition of $Y_2(CO_3)_3{\cdot}nH_2O{:}Eu^{3+}$ to form $Y_2O_3{:}Eu^{3+}$.

4. Conclusions

A new red-emitting carbonate phosphor, $Y_2(CO_3)_3{\cdot}nH_2O{:}Eu^{3+}$, was successfully synthesized via the hydrothermal route using urea as a precipitant. At low heating temperatures, spherical $Y_2(CO_3)_3{\cdot}nH_2O{:}Eu^{3+}$ particles with a micrometer size were obtained. When the temperature was increased, the size of the synthesized powders increased apparently and the morphology of the powders became a rod-like shape. The optical characteristics of the Eu^{3+} emission were observed in the region of 580–620 nm under near UV-excitation. The strongest red emission was at 615 nm due to the $^5D_0 \rightarrow {}^7F_2$ transition. The luminescent properties revealed that Eu^{3+} ions occupied 9-coordination sites in the host lattice. $Y_2(CO_3)_3{\cdot}2H_2O{:}Eu^{3+}$ was thermally decomposed at elevated calcination temperatures to form $Y_2O_3{:}Eu^{3+}$. The obtained $Y_2O_3{:}Eu^{3+}$ exhibited a rod-like morphology and an intense red emission at 611 nm.

References

[1] R.J. Yu, W.J. Ding, G.G. Zhang, J.H. Zhang, J. Wang, J. Alloys Compd. 509 (2011) L273–L278.
[2] Z.F. Wang, Y.H. Wang, Y.Z. Li, B.T. Liu, J. Alloys Compd. 509 (2011) 343–346.
[3] F.S. Chen, C.H. Hsu, C.H. Lu, J. Alloys Compd. 505 (2010) L1–L5.
[4] B.T. Liu, Y.H. Wang, F. Zhang, Y. Wen, Q.Z. Dong, Z.F. Wang, Opt. Lett. 35 (18) (2010) 3072–3074.
[5] C.F. Guo, X. Ding, H.J. Seo, Z.Y. Ren, J.T. Bai, J. Alloys Compd. 509 (2011) 4871–4874.
[6] F. Gutierrez-Martin, F. Fernandez-Martinez, P. Diaz, C. Colon, A. Alonso-Medina, J. Alloys Compd. 501 (2010) 193–197.
[7] Y.J. Zhang, M.R. Gao, K.D. Han, Z.Y. Fang, X.B. Yin, Z.Y. Xu, J. Alloys Compd. 474 (2009) 598–604.

[8] R.H. Dafinova, R.K. Stoianova, J. Mater. Sci. Lett. 6 (1987) 254–256.
[9] R. Miyawaki, J. Kuriyama, I. Nakai, Am. Mineral. 78 (1993) 425–432.
[10] C.H. Wu, F.S. Chen, S.H. Lin, C.H. Lu, J. Alloys Compd. 509 (2011) 5783–5788.
[11] C.H. Lu, B.J. Shen, J. Alloys Compd. 497 (2010) 159–165.
[12] C.T. Lee, F.S. Chen, C.H. Lu, J. Alloys Compd. 490 (2010) 407–411.
[13] M.M. Xing, W.H. Cao, H.Y. Zhong, Y.H. Zhang, X.X. Luo, Y. Fu, W. Feng, T. Pang, X.F. Yang, J. Alloys Compd. 509 (2011) 5725–5730.
[14] J. Yang, Z.W. Quan, D.Y. Kong, X.M. Liu, J. Lin, Cryst. Growth Des. 7 (4) (2007) 730–735.
[15] Y.F. Liu, Z.P. Yang, Q.M. Yu, J. Alloys Compd. 509 (2011) L199–L202.
[16] S.A. Yan, Y.S. Chang, W.S. Hwang, Y.H. Chang, M. Yoshimura, C.S. Hwang, J. Alloys Compd. 509 (2011) 5777–5782.
[17] Y.V. Yermolayeva, A.V. Tolmachev, M.V. Dobrotvorskaya, O.M. Vovk, J. Alloys Compd. 509 (2011) 5320–5325.
[18] S. Liu, R.J. Ma, R.Y. Jiang, F.C. Luo, Synth. React. Inorg. Met. 30 (2) (2000) 271–279.
[19] O.A. Graeve, J.O. Corral, Opt. Mater. 29 (2006) 24–30.
[20] W.W. Zhang, M. Yin, X.D. He, Y.Q. Gao, J. Alloys Compd. 509 (2011) 3613–3616.
[21] N. Dhananjaya, H. Nagabhushana, B.M. Nagabhushana, B. Rudraswamy, C. Shivakumara, R.P.S. Chakradhar, J. Alloys Compd. 509 (2011) 2368–2374.